Nanoscale

RSC Publishing

FEATURE ARTICLE

View Article Online
View Journal

Actuators based on liquid crystalline elastomer materials

Cite this: DOI: 10.1039/c3nr00037k

Hongrui Jiang,*[ab] Chensha Li[a] and Xuezhen Huang[a]

Liquid crystalline elastomers (LCEs) exhibit a number of remarkable physical effects, including the unique, high-stroke reversible mechanical actuation when triggered by external stimuli. This article reviews some recent exciting developments in the field of LCE materials with an emphasis on their utilization in actuator applications. Such applications include artificial muscles, industrial manufacturing, health and microelectromechanical systems (MEMS). With suitable synthetic and preparation pathways and well-controlled actuation stimuli, such as heat, light, electric and magnetic fields, excellent physical properties of LCE materials can be realized. By comparing the actuating properties of different systems, general relationships between the structure and the properties of LCEs are discussed. How these materials can be turned into usable devices using interdisciplinary techniques is also described.

Received 3rd January 2013
Accepted 4th April 2013

DOI: 10.1039/c3nr00037k

www.rsc.org/nanoscale

1 Introduction

Driven by applications, new materials are constantly being developed for enhanced performance and new functions. Among them, there is a group of materials capable of responding to external stimuli with mechanical deformation. Some so-called *smart materials* fall into this category and are of particular interest, as they may also bear structural similarities to the living systems, or to some extent, adapt in response to external stimuli. Developing these smart materials has long been recognised as an exciting and significant research area with widespread applications.[1,2] Several different types of smart responsive materials have been developed so far, with varying mechanical properties and response mechanisms. Compared with other smart materials, polymers have many advantages such as good processability, excellent corrosion resistance, light-weight, biocompatibility, and the potential to mimic the movements of organisms.[3,4] Liquid crystalline elastomers (LCEs), a type of lightly cross-linked liquid crystalline polymer (CLCP), are novel materials among the polymer smart materials. They have properties of both liquid crystals and elastomers: the self-organization nature of liquid crystal systems and the

[a]Department of Electrical and Computer Engineering, University of Wisconsin-Madison, WI 53706, USA. E-mail: hongrui@engr.wisc.edu
[b]Materials Science Program, University of Wisconsin-Madison, WI 53706, USA

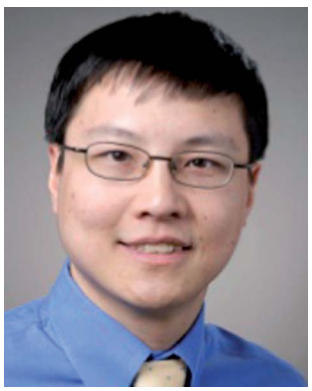

Hongrui Jiang received his Ph.D. degree in electrical engineering in 2001 from Cornell University, USA. From 2001 to 2002, he was a Postdoctoral Researcher with the Berkeley Sensor and Actuator Center, University of California at Berkeley, USA. He is currently a Vilas Distinguished Achievement Professor in the Department of Electrical and Computer Engineering, and a Faculty Member of the Materials Science Program, University of Wisconsin-Madison. He is a member of the Editorial Board of the Journal of Microelectromechanical Systems. His research interests are in microelectromechanical systems (MEMS), smart materials and micro-/nanostructures, and biomimetics and bioinspiration.

Chensha Li received his Ph.D. from Harbin Institute of Technology, China, in 2000. He was a postdoctoral researcher in the Nano-Material Center in the Department of Mechanical Engineering, Tsinghua University, China, from 2000 to 2002. From 2002 to 2005, he was an assistant professor in Tsinghua Unversity. From 2005 to 2007, he was a postdoctoral researcher in the Department of Chemical Engineering, McMaster University, Canada. From 2007 to 2012, he was a research associate in the Department of Electrical and Computer Engineering, University of Wisconsin-Madison, USA. His research interests focus on smart materials, nanotechnology and their application in microelectromechanical systems (MEMS).

flexibility stemming from the elasticity of polymer networks allow for large and reversible anisotropic dimensional changes in response to applied stimuli. Therefore, they are particularly useful and interesting materials that combine softness, elasticity, durability, light-weight, high force density, and notable mechanical strength with significant reversible actuation.[5,6]

LCEs are cross-linked polymer networks that contain rigid, anisotropic *mesogenic* units incorporated into the polymer chains.[5] Due to the anisotropic nature of these units, the materials exhibit a liquid crystalline structure in which the mesogenic units have a certain orientational order but remain individually mobile and thus could flow with respect to one another. In the nematic phase, the mesogenic units are preferentially aligned in one particular direction but have no positional order and no crystalline regularity. When these units are topologically fixed *via* incorporation into a crosslinked polymer network, an overall distortion in the dimensions of the polymer network could take place through liquid crystalline phase transition. To translate the distortion into a change in the dimensions of the bulk material, all of the mesogenic units within it need to be aligned preferentially in the same direction, the nematic *director*.[7–10] The transition between the nematic and isotropic phases may be caused by adding non-mesogenic solvents, heating, or in some cases ultraviolet (UV) irradiation. During this transition, a monodomain nematic LCE material will contract along the director. Such contraction can be quite large and reversible, making these materials great candidates as actuation materials.[11,12] The nature of the mesogenic molecules, the crosslinking degree (low or high density), and the connectivity of the mesogens (side-chain or main-chain) to the polymer backbone are factors that determine the change in length and the mechanical properties of LCEs. In 1997, de Gennes *et al.* reported on theoretical studies on the possibility of using LCEs as artificial muscles.[13,14] They proposed that a slight drop in the temperature across the isotropic (I)-to-liquid crystal (LC) transition would be able to cause a strong uniaxial deformation of LCEs at a nearly constant volume owing to a change in the LC order. Finkelmann and Kundler later reported that nematic LCE films containing polysiloxanes exhibited a spontaneous contraction along the director axis when heated towards the nematic to isotropic phase-transition temperature.[15] After this phenomenon was originally predicted by de Gennes *et al.* and experimentally confirmed by Finkelmann and Kundler, theoretical and experimental studies in this area have been expanded by many researchers. Moreover, such materials, with both rubber-like elasticity and anisotropic liquid crystalline ordering, are of tremendous interest in potential applications in industry and health. Various types of LCEs have been developed. Uniaxial deformations of well over 300% during the phase change have been demonstrated.[8] LCEs also demonstrate other interesting physical features;[16,17] however, this spontaneous reversible deformation allows a potentially large actuation stroke and currently makes them stand out from other soft actuators.

2 The synthesis and fabrication of LCE materials

The synthesis of LCEs generally requires the build-up of a LC polymer consisting of mesogenic groups and polymer chains; the crosslinking of the polymer chains forms a large network. One type of synthetic method requires the use of a solvent during the crosslinking step to ensure full miscibility and a homogeneous distribution of the reactants. A widely adopted approach is based on silicone chemistry. It starts with a linear, nonfunctional polyhydrosiloxane chain, which is coupled with mesogenic groups and a crosslinking agent in one step. The addition of terminal C=C double bonds to Si–H bonds catalyzed by platinum catalyst[18] is used to attach the mesogens and crosslinking moieties to the polyhydrosiloxane chain. Kinetic studies showed that vinyl groups react two orders of magnitude faster than methacryloyl groups. This allows the crosslinking to occur in two steps.[7] The vinyl groups react very fast, bringing about a weakly crosslinked network. The slower reaction of the methacryloyl groups in the second step leads to a full crosslinking of the sample. This method can be used in the preparation of highly oriented LCE materials. This synthetic route is very simple to perform and mesogenic compounds can be exchanged without extensive changes being made to the whole system. A huge variety of LCE samples with different mesogenic groups and crosslinking compounds can be prepared by this method. Nonetheless, the resulting elastomeric network may be difficult to purify. Low molar mass materials may remain in the elastomer owing to an incomplete reaction which might cause migration and phase separation. These impurities must be removed by extraction with a suitable solvent from the elastomer, which unfortunately is very time consuming. The second route starts with a liquid crystalline polymer that contains additional functional groups. This polymer is mixed with a bi- or multi-functional crosslinking agent that can react selectively with these functional groups under defined reaction conditions, leading to network formation.[19–23] This pathway has the advantage that the LC polymers can be purified and characterized before the crosslinking step. In another type of synthetic

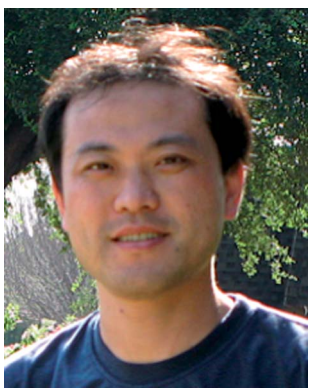

Xuezhen Huang received his Ph.D. from the Department of Chemistry in Texas Christian University (TCU), USA, in 2010. Afterwards, from 2010 to 2012, he kept working on nanofabrication, semiconductor nanomaterials and photoluminescence of rear earth elements as a postdoctoral researcher at TCU. He is currently a research associate at the Department of Electrical and Computer Engineering of University of Wisconsin-Madison, USA. His recent research interests focus on the design, synthesis and characterization of nanostructured materials for application in energy conversion and storage, biological sensors, catalysis and light-driven actuators.

method, the liquid crystalline prepolymer already contains crosslinkable groups or a liquid crystalline monomer with a polymerizable group is mixed with a radical initiator and a multifunctional crosslinker; no solvent is needed for the crosslinking reaction. The mixture can be thermally polymerized and crosslinked or by UV irradiation.[24–32] A typical example is incorporating acrylate functionalized mesogens and diacrylate functionalized crosslinkers containing photoisomerizable molecules or molecular chromophores, which are polymerized radically by thermal or UV initiation, to form a network structure.[3,6,31,33,34] This approach allows for the use of many orientation techniques known to low-molecular-weight liquid crystals before the crosslinking process.

Furthermore, LCEs have been prepared by block copolymerization[28,35] and hydrogen bonding.[36,37] The synthesis of block copolymers with well-defined structures and narrow molecular-weight distributions is a crucial step in the production of artificial muscles based on triblock elastomers. Li *et al.* proposed a muscle-like material with a lamellar structure based on a nematic triblock copolymer. The material consists of a repeated series of nematic polymer blocks and conventional rubber blocks.[28] Talroze and co-workers studied the structure and the alignment behavior of LC networks stabilized by hydrogen bonds under mechanical stress.[36] They synthesized poly[4-(6-acryloyloxyhexyloxy)benzoic acid] that exhibits a smectic LC phase over a broad temperature range. The amorphous azopyridine polymer can easily be converted into LC polymers through hydrogen bonding with a series of commercially available aliphatic and aromatic carboxylic acids.[37] The pure acids have only a crystal phase that melts at high temperatures. After mixing them with the azopyridine polymer, the complex formed shows a new LC phase. This observation is strong evidence of the formation of hydrogen bonded complexes, because neither the pure acids nor the azopyridine polymer shows any LC phase.

The main aspect of LCE material fabrication is the orientation of the mesogens to form a liquid crystalline monodomain, which is the prerequisite for actuation performances. The chains of a weakly crosslinked liquid crystalline polymer can be deformed, leading to an anisotropic environment for the mesogens. Ultimately they will adopt a regular alignment with respect to the polymer chains—an LC monodomain. On the other hand, the mesogens of a liquid crystal can be aligned uniformly with one of the well-known orientation techniques. Afterwards, the polymer network is formed in the anisotropic environment of the LC, resulting in a deformed backbone conformation. The deformation of a polymer network is usually done by mechanical stretching. To this end, a weakly crosslinked liquid crystalline polymer is synthesized and stretched uniaxially to a certain degree. This causes an unfolding of the polymer chains, against the entropy. In the LC phase, the mesogens in the polymer align themselves either parallel or perpendicular to the polymer chain, leading to a monodomain. The material is further crosslinked in the LC phase to lock in the conformation of the backbone. The precondition for this method is that the material has some mechanical stability or is at least highly viscous. A typical example is the two-step crosslinking process combined with a drawing process for polysiloxane based LCEs, which was introduced by Küpfer and Finkelmann.[7] The alignment in the LCE network is formed in the drawing process. In the first step, a well-defined weak network is synthesized, which is deformed with a constant load to induce network anisotropy. The load has to exceed the threshold load, which is necessary to obtain a uniform director orientation (monodomain). Then, a second cross-linking reaction is conducted and it locks in the network anisotropy. The resulting samples are usually optically clear and highly ordered. Another example of mechanical orientation is the drawing of fibres from a polymeric liquid crystal and a quick crosslinking afterwards, before the obtained orientation is lost. This can be manually done[20,26] or in a more sophisticated electrospinning process.[27,38] These LCEs are easily prepared and highly ordered, and to some extent mimic natural muscles.

A special kind of mechanical orientation is the use of the flow field from a fluid moving inside a confined space.[39–41] In this method, a microfluidic setup is utilized to make liquid crystalline monomeric materials flow through a thin capillary, dispersed in a carrier fluid, followed by crosslinking under UV irradiation. No pre-crosslinking is necessary because the materials do not have to be mechanically stable to be stretched. A host of micro-scale LCE particles can be made quite easily with this technique, whereby parameters such as size, shape, and actuation properties of the particles can be controlled by the microfluidic setup. Continuous LCE fibres can also be made by this method.[41]

For the reaction mixture of liquid crystalline monomers with low viscosity, monodomains of nematic LCE films can be made using alignment layers.[9,31] Typically the monomer mixture is first melted on a glass substrate coated with a rubbed polyimide film, and then cooled down into the LC phase and polymerized by UV irradiation. The mesogens in the obtained films, which can later be removed from the glass substrate, show an alignment parallel to the rubbing direction.

Other methods to form macroscopic uniaxially oriented LCE films based on the manipulation of the mesogenic units include use of magnetic and electric fields,[29,42,43] polarized light,[44,45] surface forces,[46–52] *etc.* Then cross-linking processes can form an anisotropic network if the LC mixtures contain polymerizable and cross-linkable bi-functional monomers.

3 Actuators based on LCE materials

The actuation performances of LCE materials stem from the memory effects of LC networks that are displayed in the macroscopic shape and/or dimension memory, and memory in configuration. The phase state at the time of cross-linking determines the organization of the LC elastomeric network.[53] Very large shape changes occur while translating into the isotropic state. These changes in dimension are qualitatively identical to the dimensional changes that occur when the nematic elastomers are under stress. Once the elastomer is in the mesophase, a highly aligned network could be recovered. This memory is particularly interesting because it arises from an equilibrium situation and is not due to kinetic factors. Many

of the observed properties and phenomena of LCE materials are related to the nature of the coupling between the mesogens and the polymer backbone. With these structures, a mechanical deformation of the network matrix is coupled with the orientation of the mesogenic side groups to generate much bigger effects. Conversely, a change in the orientation of the mesogenic groups driven by an external field is reflected in the deformation of the network. The nature of the relative dispositions of the backbones and the mesogenic units is controlled by the strengths of the interactions within the mesogenic units, within the polymer backbones, and between the mesogenic units and polymer backbones. The latter may be resolved into two components: one component favors parallel alignment between the mesogenic units and the polymer chains simply because of the nematic field, and the other component is related to the nature of the coupling.

The possibility of using LCEs as artificial muscles, by taking advantage of their substantial uniaxial contraction in the direction of the director axis, was proposed by de Gennes and Seances.[54] Afterwards there have been a number of efforts to develop artificial muscle-like materials.[9,20,28,55–59] Wermter and Finkelmann reported a type of LC coelastomer composed of LC side chains and LC main-chain polymers as network strands. The LCEs showed a large contraction of 300% through the phase transition.[55] Ratna and co-workers prepared LCEs with laterally attached side-chain mesogens. The LCEs showed a maximum retractive stress of 270 kPa through phase transition.[9] Naciri *et al.* developed a method for preparing LC fibers from a side-chain LC terpolymer containing two side-chain mesogens and a nonmesogenic group that acts as a reactive site for crosslinking. A retractive stress of nearly 300 kPa was also observed in the isotropic phase. These are all comparable to that of a skeletal muscle.[20]

Following the trend of miniaturization found in many fields of materials science, LCE materials have also become attractive in MEMS. They can be employed in microdevices because of their relative ease of integration and excellent mechanical properties. With the aim to apply them in such domains, advanced technologies such as soft lithography, microreplication, microfluidics, microprinting and photomasking are needed.[60]

3.1 Actuators based on thermally actuated LCE materials

Anisotropic deformation of monodomain LCEs by a thermal phase transition from an LC to an isotropic state was first reported by Küpfer and Finkelmann.[61] A nematic LCE prepared by the two-step process contracted by about 26% owing to the change in order parameter as a result of the change in molecular alignment of mesogens. The nematic LCE possesses uniaxial orientational order. The order is characterized by its principal axis (the nematic director n) and the scalar order parameter (Q), referring to the mean orientation of the mesogenic groups with respect to the director.[62] The elastic body coupled with such internal degree of freedom can be thought of as a Cosserat medium; thus the relative movement of crosslinking points provides elastic strains and forces, while the director rotation causes local torques and couple-stresses, which are both intricately connected in the overall macroscopic response of the body. The change in the degree of alignment of mesogenic rods results in spontaneous elongation or contraction of the whole network along the nematic director. When the nematic LCE is heated above or cooled down below its nematic–isotropic transition temperature (T_{ni}), the nematic order is changed, and the spontaneous uniaxial contraction/restoration of the nematic LCE along the director axis occurs. This anisotropic deformation behavior of LCEs has been a subject of extensive experimental and theoretical studies.[62–64] Warner and Terentjev established a relationship between the nematic order parameter and the effective backbone anisotropy of polymer chains forming the rubbery network. It is expressed by a dimensionless ratio of the principal step lengths parallel and perpendicular to the nematic director.[5,65] In the nematic phase, this ratio is larger than unity, while after a nematic–isotropic phase transition, this ratio approaches unity as a result of the formation of a random coil of polymer chains, which makes the polymer material contract along the director axis of LCEs.

Sánchez-Ferrer *et al.* developed thermal-actuated LCE materials which can be integrated into microsystems for actuators and micromachines.[66] A gripper was developed, and the structure and performance are shown in Fig. 1. The silicon arms were integrated and actuated by the LCE actuators. The controlled thermal actuation was induced by electric power. A gold wire was wound around the LCE film to heat it. The position of the arms could be changed by applying voltage at different rates. An electric voltage between 1.5 and 3.5 V was applied to produce a temperature increase in the surroundings of the elastomer strip and a strain leading to the contraction of the LCE, which in turn controlled the movement of the arms of the micromachine. Small changes in the LCE film produced strains of up to 150% in the microdevice and actuation stress values of 60 kPa, and thus showed the capacity to move up to 400 times its own mass with low hysteresis owing to the nematic to isotropic transformation.

Sánchez-Ferrer *et al.* demonstrated another work on integrating thermal-actuated LCE materials into a microsystem, where they developed a microvalve for microfluidics through combining classical silicon-based technology with LCE actuators for use in lab-on-a-chip devices.[67] The actuation principle was based on the expansion of the LCE in the directions perpendicular to the director and the shrinkage in the direction parallel to the director, both of which had been considered in the design of the device, based on the actuation of the LCE from the nematic to the isotropic state. The functional LCE microvalve structure was based on complementary deformations which were elongation-bending and sealing of the microchamber in the direction of the flow, with shrinkage in the other direction perpendicular to the flow upon heating. The designed structure is shown in Fig. 2.[67] The volumetric flow of the medium was guided underneath the actuator (Level 3). A small supporting structure on the chip, which was on the same level as the bearing surfaces for the two ends of the actuator (Level 2), prevented buckling in the normal direction. In this way, the actuator deformation in the main direction could not be

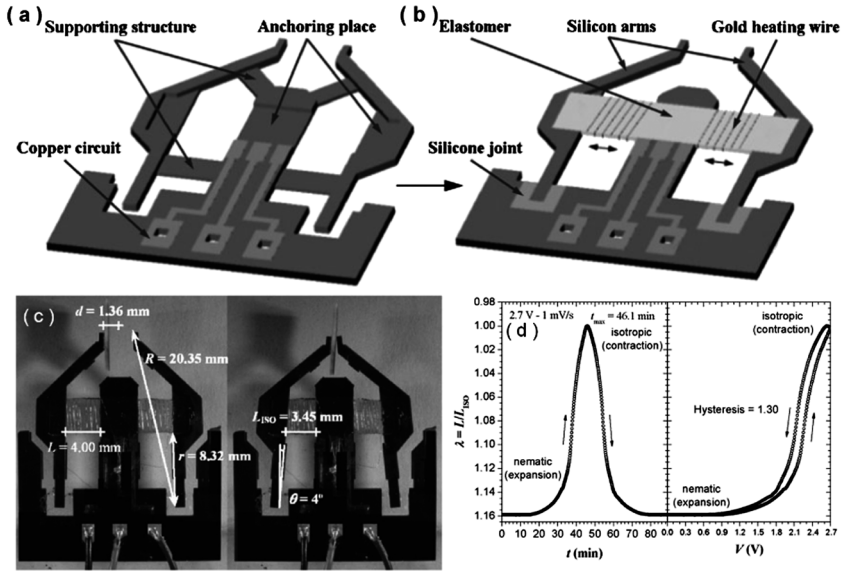

Fig. 1 An LCE actuator and its components: (a) silicon carrier during batch manufacturing, (b) elastomer mounted onto the finished gripper (elastomer dimensions: $16 \times 4 \times 0.030$ mm^3; arm length: 20 mm; frame dimensions: 22×25 mm^2). (c) Open (left) and closed (right) liquid-crystalline elastomeric microgripper on applying an electrical power, where the nematic-to-isotropic transformation induces changes of the liquid-crystalline elastomer film length that causes the strain. (d) Thermal contraction–expansion (λ) as a function of the heating–cooling time (left) and as a function of the variation of voltage (right) for the microgripper. Reprinted with permission from ref. 66. Copyright 2009, Wiley-VCH.

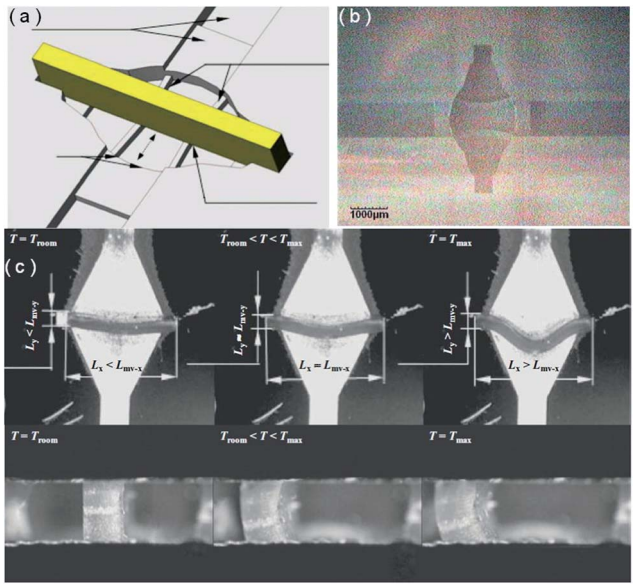

Fig. 2 (a) Solid model of a half of an LCE microvalve. (b) Top view of the microchip before assembly. (c) Snapshot pictures taken during the actuation of the LCE microvalve. The actuator pushes itself at the end of the extension into the microchannel opening: moving of the microvalve-structure before the assembly of the microchip (top), and moving of the ready LCE–silicon structure through an artificial hole on one side of the chip (bottom). Reprinted with permission from ref. 67. Copyright 2011, Wiley-VCH.

avoided and the deformation of the LCE was compensated by an elevated channel ground (Level 1). Two identical chips were assembled together face to face in one system including the elastomer actuator in between. One part of the assembled chip had a copper circuit on its back for heating; the other one had some electric contacts for temperature measurement (backside of the microchip). As shown in Fig. 2(c), when the temperature increased, the LCE microvalve filled the room in the directions perpendicular to the director (L_x and L_y), up to the wall, sealing the interior of the structure. When the tension grew, an abrupt buckling of the actuator occurred in the middle and closed the microchannel. This middle part of the actuator moved to the microchamber and blocked the flow of the fluid at the microchannel opening. The actuator then created extra pressure because of self-clamping at the two ends. The shrinkage of the actuator in the direction parallel to the director aided in its movement in the microchamber because of the friction forces being reduced between the actuator and the microstructure.

Keller *et al.* made μm sized thermal-actuated LCE actuators,[59] again demonstrating the integration of LCEs in a hybrid way for the development of microsystems. By applying the replica moulding technique to the domain of nematic LCEs, an array of nematic LCE pillar actuators was prepared. Fig. 3(a) illustrates the experimental setup used to prepare the LCE pillars.[59] The silicon template was fabricated by employing photolithography, and the soft poly(dimethylsiloxane) mould with an array of holes 20 μm in diameter and 100 μm in height was prepared by silicon template-based first replication. Then, the mould was pressed onto a melted monomer mixture consisting of a nematic side-on acrylate monomer and a cross-linker. The monomer mixture was slowly cooled to its nematic phase, and UV-light induced polymerization was performed under a magnetic field to align the nematic director parallel to the long axis of the pillars. An array of pillars of nematic LCE was thus obtained, as shown in Fig. 3(b). When heated from a nematic phase to an isotropic phase, the pillars underwent a contraction on the order of 30–40%. The contracted pillars

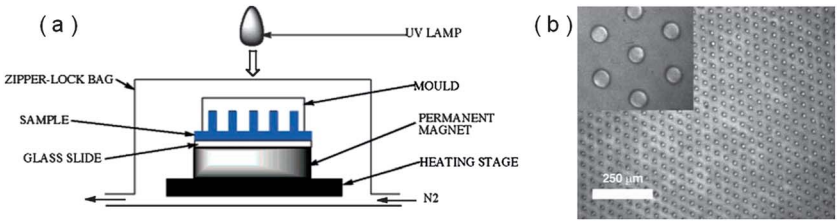

Fig. 3 Micrometer-sized nematic LCE actuators consisting of a pillar array. (a) Experimental setup used to prepare the responsive pillars. (b) Top view (under an optical microscope) of the pillar pattern obtained by the imprint in the nematic liquid crystal elastomer. (Inset) Zoom on the structure (pillar diameter = 20 μm). Reprinted with permission from ref. 59. Copyright 2006, American Chemical Society.

could revert to their original size after cooling from the isotropic phase to the nematic phase. Each pillar behaved as a small actuator, hence an array of μm sized nematic LCE actuators controlled by temperature. Such an actuator array could have potential applications in the fabrication of active surfaces where small geometric variations often result in drastic changes in the surface properties, such as roughness, wettability, adhesion.

Later in ref. 68, the same group prepared a new nematic thiol–ene monomer and a new tetrafunctional nematic crosslinker (Fig. 4(a)). Using the same setup, they obtained thin glassy polymer films covered by pillars of the nematic main-chain LCE, as explored by scanning electron microscopy (SEM; Fig. 4(b)). Those pillars, when heated above their T_{ni}, contracted reversibly by around 300 to 400%.[68] The prepared LCE micro-actuator array with ultralarge contraction paves the way for the development of LCE-based responsive surfaces mimicking natural surfaces with specific properties.

3.2 Actuators based on photo-mechanically actuated LCE materials

In recent years, photo-actuated LCE actuators have been under flourishing development, since light is a clean energy source and can be remotely, conveniently and precisely manipulated. The materials which can serve as the main driving parts of the light-driven actuators do not need the aid of batteries, electric wires and gears. Therefore, light-driven materials promise important roles in many applications.[69] Most of the photochromic molecule systems capable of generating photodeformation contain azobenzene chromophores. The reversible *trans–cis* isomerization of azobenzenes can be described as a geometrical isomerisation: upon alternate irradiation of UV (or visible light with specific wavelengths) and visible light in other spectral ranges,

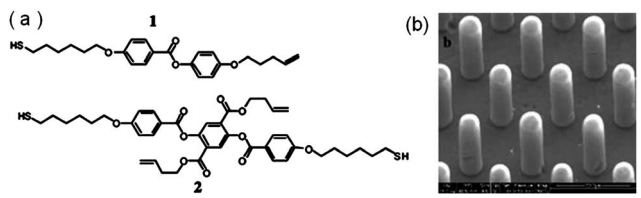

Fig. 4 (a) The nematic thiol–ene monomer and tetrafunctional nematic crosslinker used to prepare main-chain LCEs. (b) SEM image of a surface covered with cylindrical pillars. Reprinted with permission from ref. 68. Copyright 2009, American Chemical Society.

azobenzene undergoes reversible *trans–cis* isomerization accompanied by a significant change in molecular length from about 9.0 Å in the *trans* form to 5.5 Å in the *cis* form. Therefore, by incorporating azobenzene chromophores into polymer backbones of the crosslinked LC networks, irradiation at the two different wavelengths can produce reversible contraction and expansion of the materials.[70–73] Finkelmann *et al.* first reported on a synthesized LCE with an azobenzene based molecule as the mesogenic unit that led to substantial photogenerated contractile strains (~20%), arising from a decrease in the order of the LC phase.[74] Afterwards, a variety of azobenzene LCEs and LCE-type CLCPs were developed. Photo-induced bending in azobenzene CLCPs (including LCEs) has also been achieved,[6,31,33] even with precise directional control of bending,[75] ascribed to a volume contraction induced by the photochemical phase transition in the surface region of the materials. Many photo-actuated actuators were based on this type of material.

Tabiryan *et al.* developed dynamic optical systems based on deformable and optically reflective membranes and cantilevers of azo-CLCP materials with photoinduced three-dimensional (3D) bending and precise local deformation. The power of a laser beam was utilized to control the shape of a reflective azo-CLCP membrane, adjusting its curvature, which in turn modulated the reflected spot profile of the laser beam.[76] In another example, the azo-CLCP films were cut into rectangular cantilevers, and silver films were deposited on one side of the cantilevers by electrostatic adhesion. The operation of these cantilevers is shown in Fig. 5.[76] The azo-CLCP cantilevers bent away from the control laser beam, while a second laser beam focused onto the silver reflective side was used as a probe beam to characterize the photoinduced bending of the cantilevers, as shown in Fig. 5(a). The deflected angle of the probe beam varied with increasing power density of the control laser, as shown in Fig. 5(b). The process was reversible, and the initial position of the reflected probe beam was restored after the control beam was blocked. Fig. 5(c) shows the photos of the position of the probe beam reflected from a vertically mounted cantilever at different time instants during the processes of blocking and unblocking the control laser beam. It was further demonstrated that the bending of the azo-CLCP cantilevers would also be triggered by a laser beam propagating along the surface if the material was in close proximity to it.[76] These studies show the potential of integrating the light-driven LCEs into complex and functional optical systems.

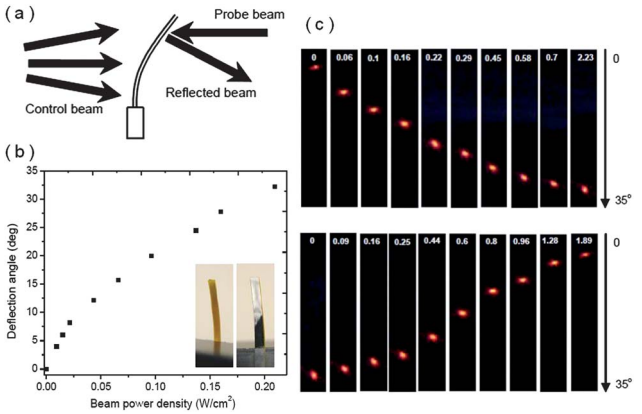

Fig. 5 (a) Schematic of the setup for demonstrating the deflection of a laser beam due to the photoinduced bending of an azo-CLCP cantilever. (b) Deflection angle of the probe He–Ne laser beam as a function of the power density of a pump Ar^+ laser beam. The inset shows the azo-CLCP film and its surface with a silver film. (c) The position of the probe laser beam reflected from the azo-CLCP surface with the silver film at different time moments upon (top) unblocking and (bottom) blocking of the laser beam, upper numbers correspond to time in seconds. Reprinted with permission from ref. 76. Copyright 2009, Optical Society of America.

van Oosten *et al.* integrated the synthesis of photo-responsive azo-CLCPs into a microsystem.[32] They used reactive liquid crystal monomer inks and an inkjet printer to produce microactuators in the form of artificial cilia. The ink-jetted cantilevers consisted of two different CLCPs arranged in tandem with a splayed orientation, as shown in Fig. 6. Each material was sensitive to a different wavelength of light, allowing differentiated addressing of two different bending motions. Hence, activating these two parts in sequence using the two different light wavelengths would imply that the motion of the cilia is non-reciprocal, but is fully driven by light.[32] This work is promising for the functions of pumping and mixing in microfluidic systems.

Zhu *et al.* developed a light-driven micropump based on the actuator material synthesized by incorporating azobenzene moieties into a cross-linked LC network.[77] The structure of the photo-activated micropump experimental prototype is shown in Fig. 7. It mainly includes a photodeformable actuator film, a pump membrane, a pump chamber, and pipes. The plates which formed the pump were made of polymethylmethacrylate. Water was the pump medium, and the valves of the pump prototype were removed and the inlet was blocked. Therefore, the output volume should be that of the water pumped in a stroke. The photodeformable actuator film showed periodical bending and unbending upon the irradiation of UV light and visible light; correspondingly the membrane showed periodical reciprocating movements at the stimulation of the deformation of the actuator material. Upon irradiation of UV light, the difference in the contraction ratio through the thickness gave rise to the downward bending of the film, resulting in the reduction in the volume of the pump chamber. Therefore, overpressure was generated in the pump chamber and the fluid flowed into the outlet pipe. Upon irradiation of visible light, the upward unbending of the film led to the expansion of the pump chamber. Under pressure in the chamber drove the fluid to flow through the inlet valve into the chamber. The repetitive cycle could thus realize the one-way pumping of the liquid.[77] This study proves that the photoresponsive azo-contained CLCP materials have the capability to drive a micropump.

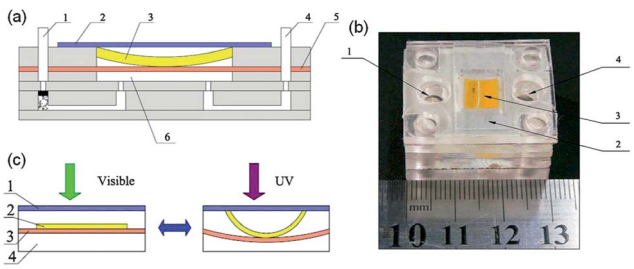

Fig. 7 (a) A schematic representing the assembled prototype of a micropump. (b) Photo of the experimental prototype ((1) inlet, (2) press plate, (3) photo-deformable material, (4) outlet, (5) pump membrane, and (6) pump chamber). (c) The photodeformable film on the pump membrane ((1) press plate, (2) photo-deformable film, (3) pump membrane, and (4) pump chamber). Reprinted with permission from ref. 77. Copyright 2010, Springer-Verlag.

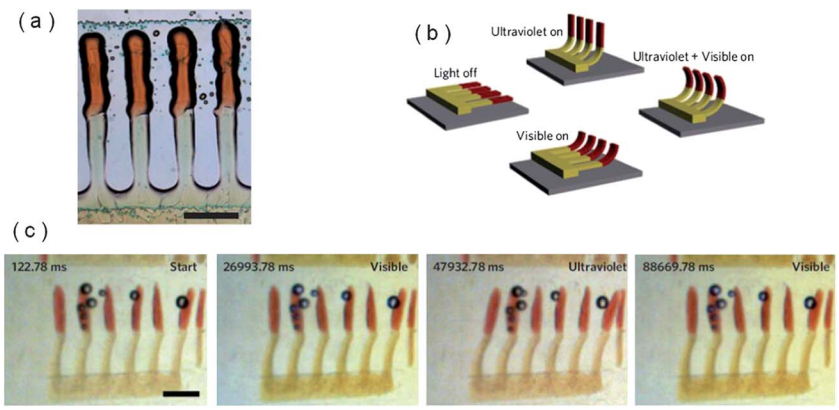

Fig. 6 (a) Cilia are made with two separate parts of CLCPs by separately polymerizing the two parts. (b) Schematic representation of light-driven cilia producing an asymmetric motion controlled by the spectral composition of the light. (c) Frontal view of actuation of multicolour cilia in water addressed with visible (4 mW cm^{-2}) and ultraviolet (9 mW cm^{-2}) light. All scale bars indicate 0.5 mm. Reprinted with permission from ref. 32. Copyright 2009, Macmillan Publishers Ltd.

Benefiting from the photo-induced deformation of the azo-CLCP materials and their ability to drive the flow of fluids under deformation, Wu *et al.* developed an adaptive liquid lens actuated by an azo-CLCP material.[78] As shown in Fig. 8, the lens cell consisted of a top glass substrate and a bottom plastic slab with two holes: a reservoir hole and a lens hole, which were sealed with elastic membranes. A photo-sensitive CLCP was attached to the membrane of the reservoir hole. Under the irradiation of a laser at a specific wavelength, the CLCP bent, exerting a pressure to regulate the curvature of the membrane at the lens hole and then changed the focal length of the plano-convex lens. The focal length was tunable from infinity to 21.2 mm in seconds. This approach paved a way to integrate CLCP actuators into compacted optical components.

Ikeda *et al.* further demonstrated light-induced rotation based on azo-containing LCE films at room temperature.[79] They prepared continuous rings by connecting both ends of the LCE films, in which azo mesogens were homogeneously aligned along the circular direction of the rings. Upon simultaneous irradiation with UV light and visible light, the ring rolled intermittently towards the light source, resulting in an almost 360° roll at room temperature. To improve the mechanical properties of azo-containing LCEs, they prepared a plastic belt of the LCE-laminated films by attaching LCE films on a flexible polyethylene sheet, and then placed the belt on a homemade pulley system. As shown in Fig. 9, upon irradiation of the belt with UV light from top right and visible light from top left simultaneously, a rotation of the belt was induced to drive the two pulleys counterclockwise at room temperature. This was the first realization of light-driven plastic motors, which directly converted photon energy to create rotational motion with soft materials. It is believed that the sections that were exposed to light expanded while those regions away from the light contracted, generating an overall rotating moment of the plastic films.

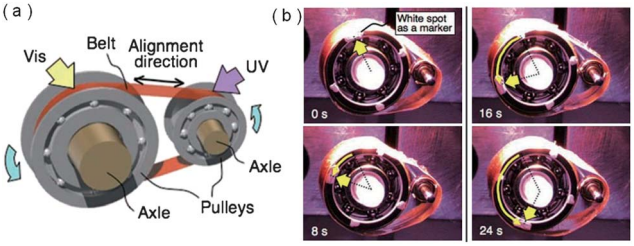

Fig. 9 A light-driven plastic motor with an LCE laminated film. (a) Schematic illustration of a light-driven plastic motor system, showing the relationship between light irradiation positions and rotation direction. (b) Series of photographs showing time profiles of the rotation of the light-driven plastic motor with the LCE laminated film induced by simultaneous irradiation with UV (366 nm, 240 mW cm^{-2}) and visible light (>500 nm, 120 mW cm^{-2}) at room temperature. Reprinted with permission from ref. 79. Copyright 2008, Wiley-VCH.

Inspired by nature, propulsion systems from photo-actuated CLCP materials have been developed. Palffy-Muhoray *et al.* presented studies of an azo dye-doped LCE film swimming on a water surface.[80] Their study demonstrated that the mechanical deformation of an LCE sample in which azobenzene dyes are dissolved in response to non-uniform illumination by visible light becomes very large (the sample bent by more than 60°). When laser light was shone from above onto a dye-doped LCE sample floating in water, the LCE swam away from the laser beam—the action resembled that of a flatfish, as shown in Fig. 10. Taking advantage of alternating bending and stretching of azo-CLCP materials upon UV and subsequent visible light irradiation, Ikeda *et al.* developed CLCP-laminated polyethylene

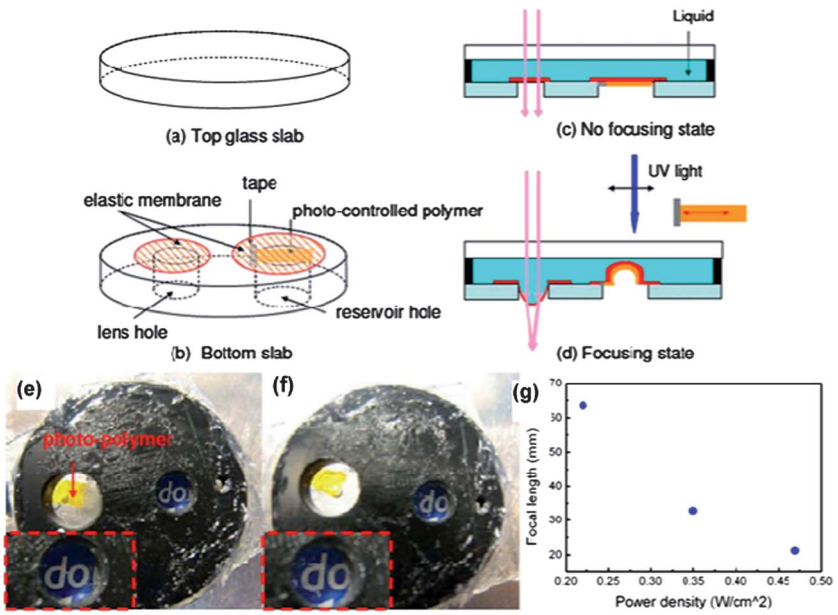

Fig. 8 A tunable lens actuated by a photo-polymer: (a) top glass slab; (b) bottom glass slab; side views of the lens cell in (c) non-focusing and (d) focusing states; (e) liquid lens in the non-focusing state; (f) liquid lens in a focusing state; and (g) measured focal length of the lens at different power densities of stimulating light. Reprinted with permission from ref. 78. Copyright 2009, OSA.

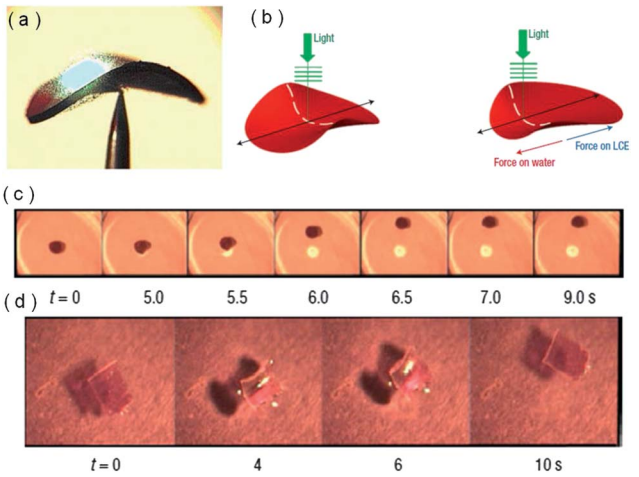

Fig. 10 An LCE film that can swim on a water surface. (a) A single video frame showing the shape deformation of an LCE sample immediately following illumination. (b) Illustration of how the sample shape changes and hence interacts with the fluid below it. The left figure shows the initial deformation of the sample on illumination. (c) A series of video frames as the LCE sample moves away from the area of sustained illumination. (d) Irregular rectangular LCE sample floating in ethylene glycol first folds and then swims away when illuminated. Reprinted with permission from ref. 80. Copyright 2004, Macmillan Publishers Ltd.

(PE) films which exhibited photomobility – sophisticated 3D motion.[81] Fig. 11(a) demonstrates a unidirectional motion, an inchworm walk, of the CLCP-laminated film with asymmetric end shapes. The film moved forward upon alternating irradiation with UV and visible light at room temperature. A close inspection of this inchworm walk revealed that upon exposure to UV light, the film extended forward because the pointed edge acted as a stationary point, and the film retracted from the rear side upon irradiation with visible light because the flat edge acted as the stationary point, which enabled the film to move in one direction only (Fig. 11(b)).

Ikeda *et al.* also utilized such CLCP-laminated films to develop a flexible robotic arm.[81] They prepared a rolled-up film by laminating with azo-CLCP layers at two places as shown in the first frame of Fig. 12. The azobenzene mesogens were aligned along the long axis of the film. The robotic arm underwent a sequential, flexible motion under light at room temperature. As shown in Fig. 12, upon exposure to UV light, the CLCP laminated part extended from a curved shape to a flat one and reverted to its initial state upon irradiation with visible light, functioning as a "hinge joint", which led to a large and flexible movement of the whole film. By controlling the irradiation position and intensity, the film could be driven in a chosen manner to manipulate objects. Yu *et al.* then developed a prototype of fully plastic microrobots.[82] The mobile parts of the microrobot were assembled with CLCP-laminated films with different shapes, which also consisted of an azo-contained CLCP layer and a PE layer. The microrobot composed of a "hand", a "wrist" and an "arm" was realized by the combination of the CLCP/PE bilayer films with different initial shapes and photodeformation modes. The photographs and the illustrations in Fig. 13 show the microrobot picking up, lifting, moving, and placing the object into a nearby container by turning on and off the light (470 nm, 30 mW cm^{-2}). First, the "hand" opened upon irradiation of light. Second, the light source was adjusted to irradiate the "wrist" instead, making the "hand" approaching the object when the "wrist" bent towards the left

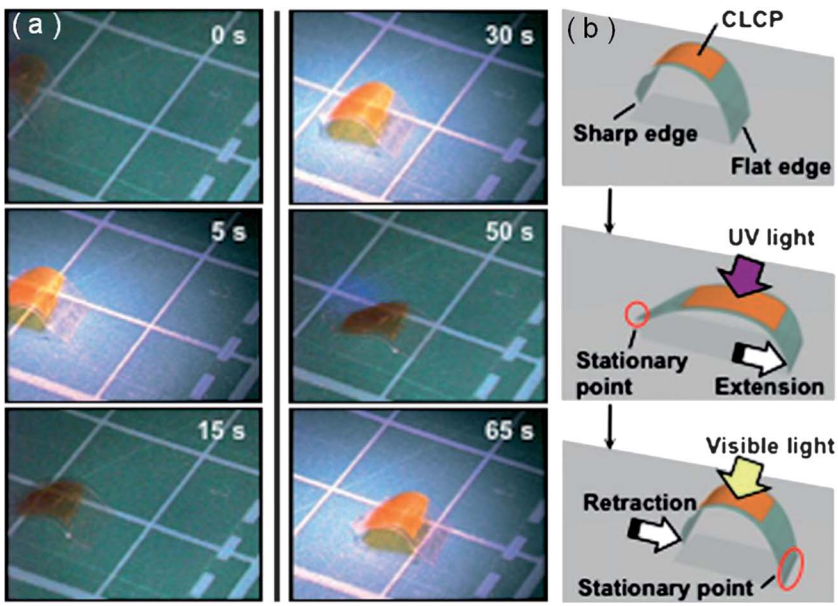

Fig. 11 A unidirectional motion of a CLCP sample, mimicking an inchworm walk. (a) Series of photographs showing time profiles of the photoinduced inchworm walk of the CLCP-laminated film by alternate irradiation with UV (366 nm, 240 mW cm^{-2}) and visible light (>540 nm, 120 mW cm^{-2}) at room temperature. (b) Schematic illustrations showing a plausible mechanism of the photoinduced inchworm walk of the CLCP laminated film. Upon exposure to UV light, the film extends forward because the sharp edge acts as a stationary point (the second frame), and the film retracts from the rear side by irradiation with visible light because the flat edge acts as a stationary point (the third frame). Reprinted with permission from ref. 81. Copyright 2009, The Royal Society of Chemistry.

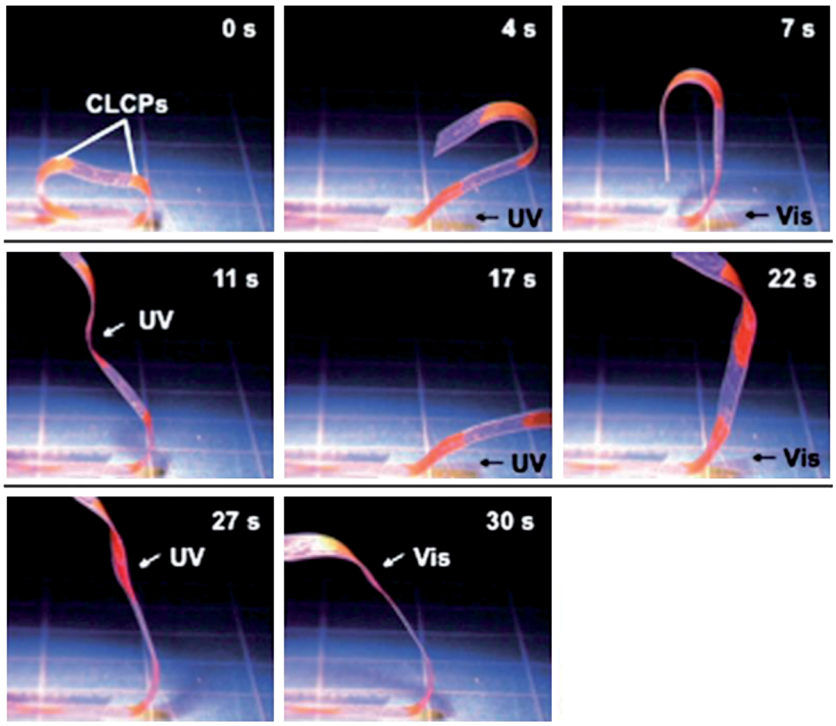

Fig. 12 Series of photographs showing time profiles of the motion of a flexible robotic arm of a CLCP laminated film induced by irradiation with UV (366 nm, 240 mW cm^{-2}) and visible light (>540 nm, 120 mW cm^{-2}) at room temperature. Arrows indicate the direction of light irradiation. Reprinted with permission from ref. 81. Copyright 2009, The Royal Society of Chemistry.

side. After the light was turned off, the "hand" closed and grasped the object. The "arm" was then irradiated with light after the object was firmly held by the "hand". Due to the bending of the "arm" towards the right side, the object was successfully lifted and moved above the container. Finally, the object was placed into the container when the "hand" opened again upon the second irradiation with light on its back. Compared to conventional electric-field-controlled robots, this kind of light-driven, fully plastic microrobots boast simple assembly and easy control and operation since electrodes for actuation are not necessary.

Based on the fast photo-response of azo-CLCP materials, Tabiryan and Bunning *et al.* developed a cantilever oscillator driven by light.[83] As shown in Fig. 14, the oscillation frequency, driven with a focused 100 mW laser with wavelengths of 457 nm, 488 nm and 514 nm, was as high as 270 Hz and was shown to be strongly correlated with the physical dimensions of the cantilever. Such high speed and oscillatory photo-driven transducers are promising for developing photo-controlled micromachines.

The photo-controlled CLCP (including LCE) actuators described above are based on photo-responsive CLCP materials developed by introducing photochromic groups into the LC networks. Light can conveniently manipulate order–disorder and order–order changes of CLCP materials, generating precise and rapid photomechanical and photomobile effects on the macroscopic scale, which are competitive and promising for many applications as soft actuators. In spite of many merits, these CLCP materials might have some inherent limits: light generally can only penetrate the surface layer of the material, and essentially only the surface chromophores can receive the light stimulus and generate actuation. Therefore, the materials are usually made in the form of thin films with the thickness within several tens of micrometers. Moreover, the photo-mechanical actuation is induced by light with specific wavelengths, while light with other wavelengths may influence adversely the photo-mechanical actuation. For example, although some photo-mechanical CLCPs can be actuated using sunlight, the driving light must first be filtered out to the desired wavelength from the wide spectrum of sunlight, followed by concentration with lenses before it can be used to actuate the materials.[84]

3.3 Actuators based on photo-thermo-mechanically actuated LCE materials

The incorporation of nano-phase materials into LCEs has been of considerable interest in recent years.[85] Aiming to achieve remote light-controlled actuation of LCE materials with a faster response time and better control, the nano-phase materials selected for LCE composites must possess special optical, thermal and physicochemical properties. Carbon nanotubes (CNTs) are one of the effective filling materials for nano-composites owing to their one-dimension structures, nano-meter-scale diameters, high aspect ratios, large surface areas, and excellent conductivities and other physical and mechanical properties.[86–88] CNTs, especially the single-wall carbon nano-tubes (SWCNTs), show strong absorptions in the visible and

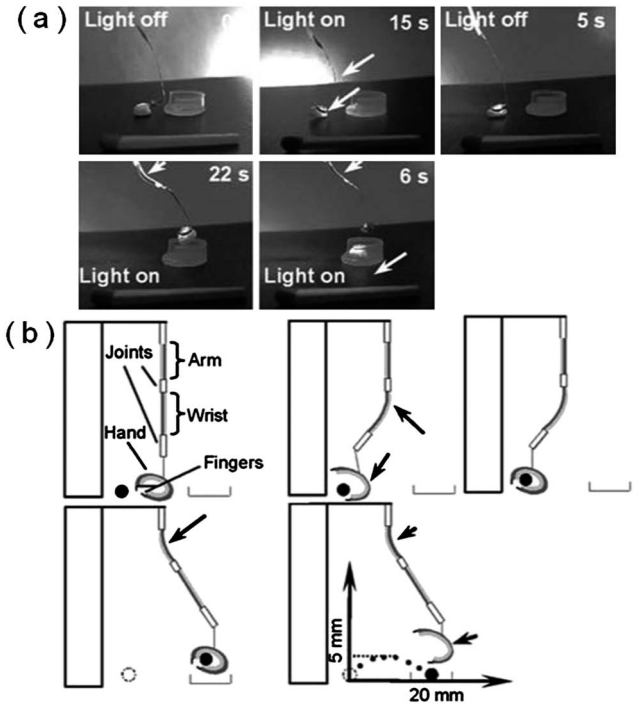

Fig. 13 A CLCP-based microrobot. (a) Photographs showing the microrobot picking, lifting, moving, and placing an object in a nearby container by turning on and off the light (470 nm, 30 mW cm^{-2}). Length shown in the pictures: 30 mm. Object weight: 10 mg. (b) Schematic illustrations of the states of the microrobot during the process of manipulating the object. The inset coordinate indicates the moving distance of the object in vertical and horizontal directions. White and black arrows denote the parts irradiated with visible light. Reprinted with permission from ref. 82. Copyright 2010, The Royal Society of Chemistry.

near-infrared (IR) regions owing to band gap transitions.[89] They can efficiently absorb and convert photon energy into thermal energy, and can serve as a nanoscale heat source and a thermal conduction pathway to heat the matrices effectively. Hence, CNTs can offer superior opportunities for the photo-actuation of thermal responsive materials. In the few recent years, some researchers successfully developed LCE nanocomposites formed by incorporating CNTs into the matrices of nematic LCEs.[90–96] The photo-thermo-mechanical actuation is realized through CNTs efficiently absorbing and converting photon energy into thermal energy, thus acting as a nano-scale heat source and thermal conduction pathway to effectively heat the LCE matrices, elevating their temperature to above the T_{ni}, changing the nematic order, and causing a reversible axial contraction and mechanical actuation. This type of LCE material is capable of utilizing the photon energy of various wavelengths simultaneously, from IR to visible light, to realize photo-thermo-mechanical actuation. Their photo-thermo-mechanical actuation has no specific spectrum dependence,[94] and thus can fully utilize the energy from a wide-spectrum light source for mechanical actuation. They can even be directly actuated by the natural sunlight.[96]

Camargo *et al.* first fabricated an effective actuation structure based on a photo-thermo-mechanically actuated LCE–CNT nanocomposite.[95] They developed a method to create sufficiently well-aligned LC units to produce localised actuation on the millimeter scale, using a moulding process to pattern features such that the actuation vector could lie in the direction normal to the surface of the pattern. It was realized to stretch and optically drive an LCE–CNT nanocomposite film within a localised area; the walls of the stretched part of the film contained aligned LC domains, while the rest of the film was a polydomain LCE. Fig. 15(a) illustrates the localised structuring process. Fig. 15(b) is a 3D illustration of the cross-section of one structured feature on a support substrate, with no applied light source. The stretched part of the crosslinked film contracted when the light source was on (Fig. 15(c)), causing a decrease in the height of the actuating features. The photo-image of the fabricated "dome-shaped" dot array pattern in an LCE–CNT nanocomposite film and the illustration of its photo-actuation

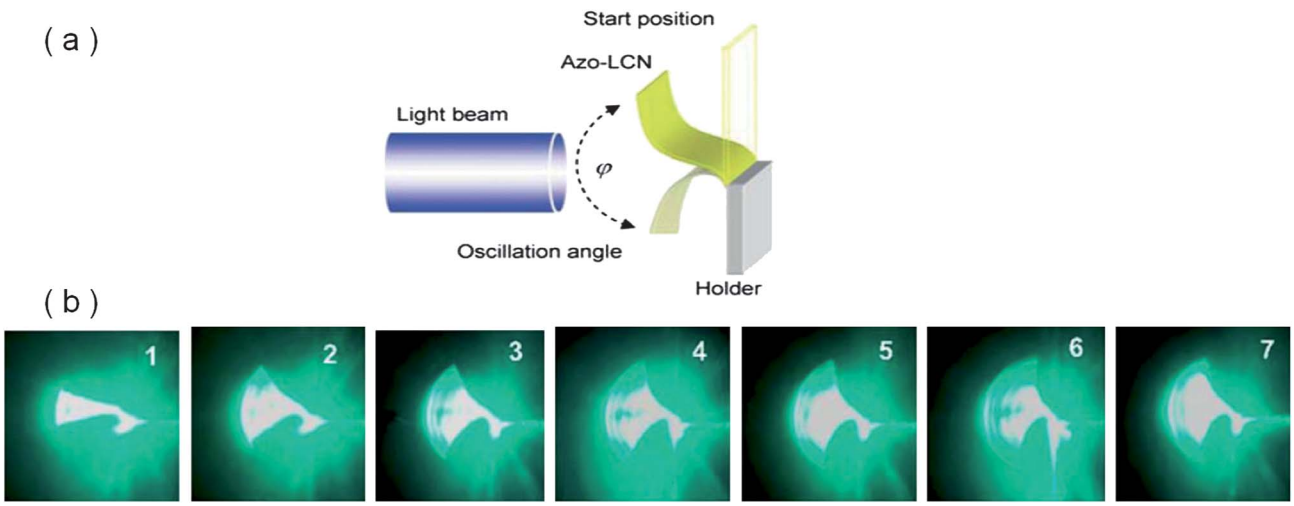

Fig. 14 A photo-driven oscillator. (a) A CLCP film is mounted vertically (starting position shown with dashed lines) and oscillates around the horizontal plane of incidence of the laser beam with full oscillation angle. (b) Snapshots of the oscillating azo-CLCP at different power levels: (1) 76 mW, (2) 85 mW, (3) 90 mW, (4) 100 mW, (5) 107 mW, (6) 121 mW, and (7) 143 mW. Reprinted with permission from ref. 83. Copyright 2010, The Royal Society of Chemistry.

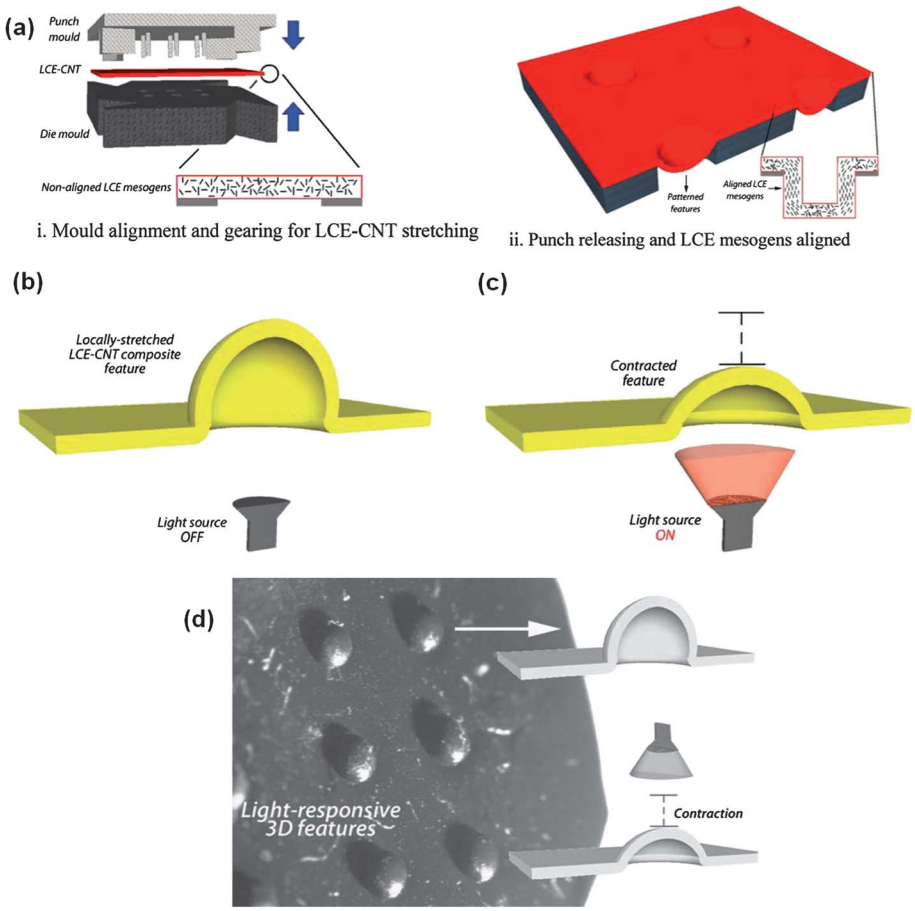

Fig. 15 Actuation based on an LCE–CNT composite. (a–c) Localised structuring process and actuation scheme of the LCE–CNT composite. (a) Structuring and stretching sequence: (i) mould alignment and gearing and LCE–CNT stretching; (ii) punch releasing and LCE mesogen alignment (mesogens are drawn as lines). (b) Ambient state, light source is off. (c) Actuated state: feature contracts when the light is on. (d) Optical stereoscopic picture of a strip of the stretched LCE–CNT composite, where the stamping process pushes the composite out of the die mould to form the "bubbled" pattern. Inset: 3D topographic change of the "bubble" under photo-actuation. Reprinted with permission from ref. 95. Copyright 2011, Wiley-VCH.

are shown in Fig. 15(d). The photo-thermo-mechanical actuation of the LCE–CNT nanocomposite was locally induced in the regions where the material had been mould-stretched, proving that only the walls of the patterned section of the film contained aligned LCE units, whereas the rest of the film remained a polydomain LCE. Such reversible, local actuation might be applied in refreshable display systems and tactile devices (*e.g.*, Braille).[95]

For the photo-thermo-mechanically actuated LCE nanocomposites, the mechanism lies in that the incorporated nanophase materials absorb and convert photon energy into thermal energy and conduct thermal energy over the matrices to heat the materials. Compared to those photo-mechanically actuated LCEs whose actuations are induced by the photoresponse of the incorporated photochromic groups, the actuation can generally be generated deeper in the materials. Hence, the materials can be made into thicker films, to about 1 mm.[92,96] As a result, a larger actuation power can be obtained. This property could make photo-thermo-mechanically actuated LCE nanocomposites more suitable for many engineering applications.

Inspired by the intriguing attribute of some plants whose leaves or flowers can follow the sun for increased light interception, called heliotropism, Jiang *et al.* developed an artificial

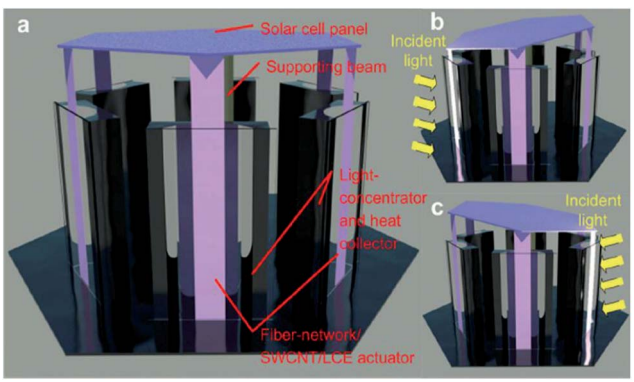

Fig. 16 Concept of artificial heliotropism. (a) 3D schematic of the system. (b and c) 3D schematic of the heliotropic behavior. The actuator(s) facing the sun contracts, tilting the solar cell towards sunlight. Reprinted with permission from ref. 96. Copyright 2012, Wiley-VCH.

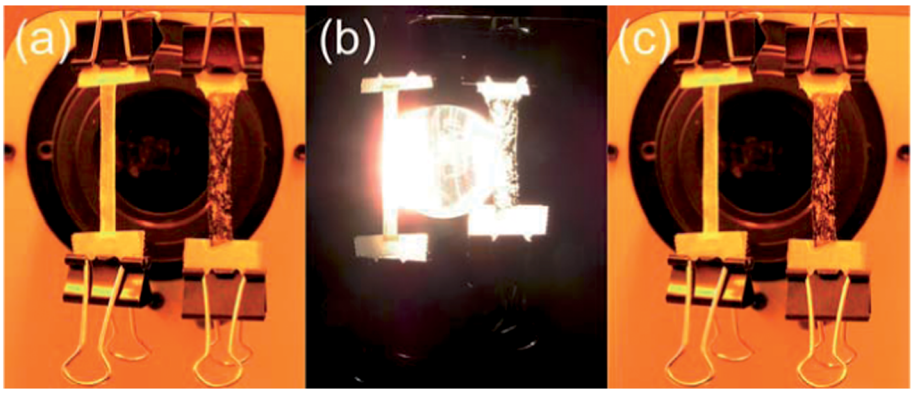

Fig. 17 Optical images of photo-actuation of a blank LCE and an SWCNT–LCE nanocomposite film. The films have dimensions of 4 cm × 0.5 cm × 0.7 mm. The irradiation intensity of the white light is 230 mW cm^{-2}. (a) The initial state of the blank LCE and SWCNT–LCE nanocomposite films. (b) Comparison of the two films under irradiation. The blank LCE does not deform after being illuminated for several minutes. In contrast, the SWCNT–LCE nanocomposite film starts to contract conspicuously after about 5 seconds, and reaches the stable length, which is about 2/3 of the initial length, after about 10 seconds. (c) The SWCNT–LCE nanocomposite film recovers to its initial length in about 9 seconds after the light source is switched off. Reprinted with permission from ref. 92. Copyright 2011, The Royal Society of Chemistry.

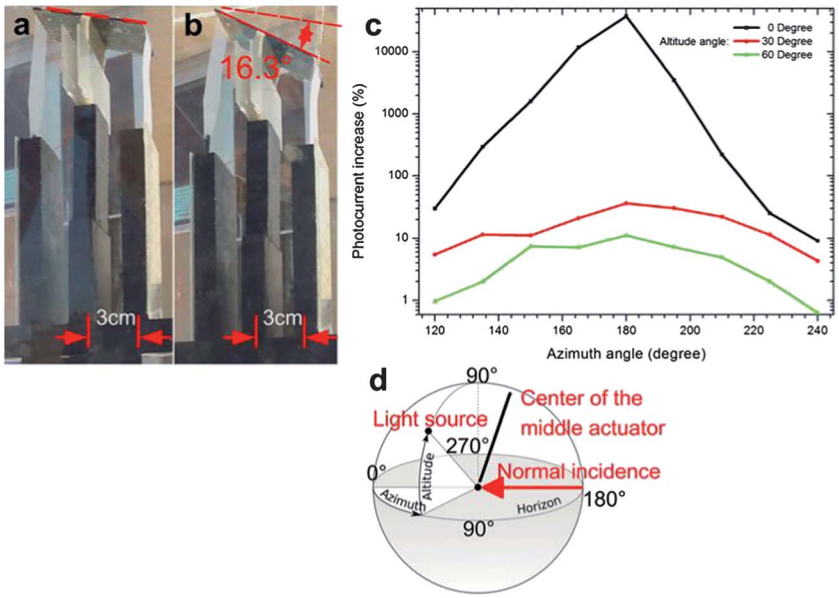

Fig. 18 Heliotropic behavior of a 2-actuator-unit device in an in-field test (a and b) and resultant photocurrent increase (c). Initially the device was blocked from sunlight. (a) The actuator was just exposed to sunlight and began to contract. (b) After 110 s, the actuator reached full contraction and the solar cell was tilted by 16.3°. (c) Photocurrent increase owing to artificial heliotropism with a single actuator unit. The incident light was kept at 100 mW cm^{-2} but was from different directions. (d) The altitude–azimuth coordinate system used. The origin was the center of the actuator facing the light. The normal incidence direction was 0° altitude, 180° azimuth. Reprinted with permission from ref. 96. Copyright 2012, Wiley-VCH.

heliotropic system for solar energy harvesting based on the photo-thermo-mechanical LCE–CNT nanocomposites.[96] The concept of the artificial heliotropism is shown in Fig. 16. At any given time instant, actuator(s) facing the incoming sunlight would be stimulated into the contracted state, while other actuators not exposed to sunlight would be in the relaxed state. Consequently, the platform supported by actuators and holding the solar cells would be driven by the contracted actuator(s) and self-adaptively tilt towards sunlight, hence the artificial heliotropism and increased photocurrent output from the solar cells. These actuators were made of photo-thermo-mechanically actuated LCE–CNT nanocomposites. In order to realize sunlight driven actuators for the artificial heliotropism, the authors developed an LCE nanocomposite by incorporating SWCNTs into a matrix of nematic LCE.[96] This LCE nanocomposite was capable of utilizing the wide spectrum of white light to realize photo-thermo-mechanical actuation,[92] as shown in Fig. 17. Moreover, the incorporation of SWCNTs into this LCE matrix significantly decreases the T_{ni} of the material, thus lowering the threshold for its photo-thermo-mechanical actuation.[92] These two factors therefore enabled the actuation of the LCE nanocomposite by natural sunlight. In order to enhance the

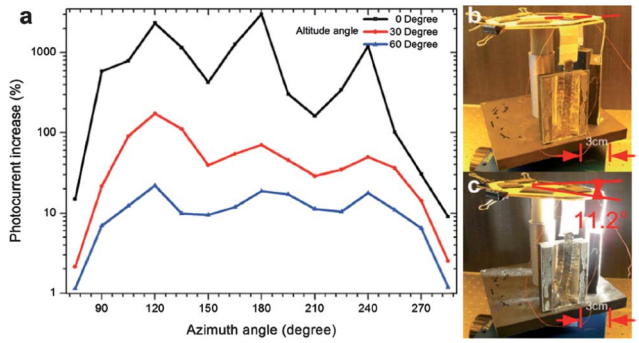

Fig. 19 Photocurrent increase owing to artificial heliotropism by a prototype device with 3-actuator units (a) and its heliotropic behavior in laboratory (b and c) tests. An altitude–azimuth coordinate system similar to Fig. 18(d) was used for data acquisition for (a). The origin was the center of the actuator in the middle. Irradiation was from a white light source (intensity: 100 mW cm^{-2}; partially collimated; spot diameter: 101.6 mm; 0° altitude; 180° azimuth) for (b and c). (b) Before irradiation. (c) 30 s after irradiation. Reprinted with permission from ref. 96. Copyright 2012, Wiley-VCH.

mechanical strength of the actuator material, the LCE–SWCNT nanocomposites were incorporated with a polyurethane fiber-network to form fiber-network–SWCNT–LCE nanocomposite strips.[96] With the auxiliary accessories performing light concentration and heat collection,[96] fiber-network–SWCNT–LCE nanocomposite actuators could be effectively actuated by the natural sunlight. The resultant artificial heliotropic devices could follow the sun for increased light interception, showing effective heliotropism in both in-field and laboratory tests, as shown in Fig. 18 and 19, respectively. As a result, a significant increase in the photocurrent output from the solar cells in the artificial heliotropic devices was observed. The mechanism of the artificial heliotropism was realized *via* direct actuation by sunlight, eliminating the need for additional mechatronic components and resultant energy consumption.[96]

4 Summary

LCEs are particularly promising materials for artificial muscles, micro-robots and MEMS. In these systems not only 2D but also 3D motion has now been achieved, and a variety of actuation modes have been developed, which are competitive and promising for many applications as soft actuators.

Of the LCE soft actuators reviewed here, some are based on thermally actuated LCEs. They possess large contraction ratios. The actuation can be uniformly generated in the body of the material, thus taking full advantage of the actuation ability of the whole material. Thermal sources are widely and conveniently available; many other forms of energy can be converted into thermal energy. Thermal energy can also be applied across large areas to simultaneously drive multiple thermally actuated LCE actuators. These merits are attractive in many applications. At the same time, photo-actuated materials are of great interest because light is an efficient and powerful source. Photo-actuated materials can realize a direct, contactless conversion of photon energy into mechanical motion, and light as the triggering source can be localised spatially and temporally, in a selective and non-damaging manner, and allows for remote activation and remote delivery of energy to a system. Therefore, more actuators based on photo-actuated LCEs have been developed. The azobenzene chromophore is an important molecular switch, exhibiting a rapid and reversible photo-isomerization that induces a reversible change in the geometry. This motion has been exploited in photo-mechanical LCE materials through crosslinking in LC networks; the LC ordering is fixed in 3D networks, giving rise to photomechanical and photomobile effects on the macroscopic scale. Photo-mechanical LCE actuators can directly convert light into mechanical energy. Owing to their sensitive photo-response and rapid and precise photoinduced actuation, they are suitable for use in micro-devices or -machines. At the present time their efficiency for light energy conversion is, however, not optimal. One reason is that the photo-mechanical actuation of this category of LCEs can only be induced by light with specific wavelengths. Another reason is that light generally only penetrates the surface layer of the materials; therefore almost only the surface chromophores can receive the light stimulus and generate actuation. For these reasons, the materials are generally made as thin films several tens of micrometers or less in thickness, which could limit the total actuation force. Some researchers have investigated on how to enhance the actuation ability of the materials themselves to overcome this problem. Ikeda *et al.* developed an azo-CLCP with a maximum contractive stress of 2.5 MPa under photo-actuation.[97] Peng *et al.* developed a homeotropic azo-CLCP incorporated with arrayed CNTs; the released stress under photo-actuation achieved a value of 26 MPa.[98] These developments are promising for effectively enhancing the actuation force of the CLCP materials. Current thermally actuated LCE matrices, while promising in their own right, generally have stresses below 1 MPa during actuation. In order to combine the merits of thermally actuated LCEs and photo-mechanically actuated LCEs, photo-thermo-mechanically actuated LCE materials have been developed in recent years. These materials have also demonstrated performances of wide appeal to engineering applications. Many challenges still lie ahead, such as the rate and precision of the photo-actuation, which are currently inferior to photo-mechanical LCEs. Many aspects of the LCE materials, such as rapid and precise photo-actuation, low threshold for response, large deformation, strong actuation force, fatigue resistance, and biocompatibility, call for further research.

Acknowledgements

This work was partially supported by the US National Institutes of Health (Grant no. 1DP2OD008678-01) and partially by the Wisconsin Alumni Research Foundation (WARF). The authors would like to express their sincere regrets to all researchers whose relevant work could not be discussed and cited in this article due to limited space.

References

1 L. Ionov, *J. Mater. Chem.*, 2010, **20**, 3382.
2 A. Lendlein, *J. Mater. Chem.*, 2010, **20**, 3332.

3 Y. Yu and T. Ikeda, *Angew. Chem., Int. Ed.*, 2006, **45**, 5416.
4 F. Cheng, Y. Zhang, R. Yin and Y. Yu, *J. Mater. Chem.*, 2010, **20**, 4888.
5 M. Warner and E. M. Terentjev, *Liquid Crystal Elastomers*, Oxford University Press, Oxford 2003.
6 H. Yu and T. Ikeda, *Adv. Mater.*, 2011, **23**, 2149.
7 J. Küpfer and H. Finkelmann, *Makromol. Chem., Rapid Commun.*, 1991, **12**, 717.
8 A. R. Tajbakhsh and E. M. Terentjev, *Eur. Phys. J. E: Soft Matter Biol. Phys.*, 2001, **6**, 181.
9 D. L. Thomsen, P. Keller, J. Naciri, R. Pink, H. Jeon, D. Shenoy and B. R. Ratna, *Macromolecules*, 2001, **34**, 5868.
10 E. M. Terentjev, *J. Phys.: Condens. Matter*, 1999, **11**, R239.
11 M. Hebert, R. Kant and P.-G. de Gennes, *J. Phys. I*, 1997, **7**, 909.
12 M.-H. Li and P. Keller, *Philos. Trans. R. Soc., A*, 2006, **364**, 2763.
13 P.-G. de Gennes, M. Hebert and R. Kant, *Macromol. Symp.*, 1997, **113**, 39.
14 P.-G. de Gennes and C. R. Acad, *C. R. Acad. Sci., Ser. IIb: Mec.*, 1997, **324**, 343.
15 I. Kundler and H. Finkelmann, *Macromol. Chem. Phys.*, 1998, **199**, 677.
16 P. Xie and R. B. Zhang, *J. Mater. Chem.*, 2005, **15**, 2529.
17 C. Ohm, M. Brehmer and R. Zentel, *Adv. Mater.*, 2010, **22**, 3366.
18 H. Finkelmann and G. Rehage, *Makromol. Chem., Rapid Commun.*, 1980, **1**, 31.
19 R. Zentel and M. Benalia, *Makromol. Chem.*, 1987, **188**, 665.
20 J. Naciri, A. Srinivasan, H. Jeon, N. Nikolov, P. Keller and B. R. Ratna, *Macromolecules*, 2003, **36**, 8499.
21 Y. Xia, R. Verduzco, R. H. Grubbs and J. A. Kornfield, *J. Am. Chem. Soc.*, 2008, **130**, 1735.
22 R. Zentel, G. F. Schmidt, J. Meyer and M. Benalia, *Liq. Cryst.*, 1987, **2**, 651.
23 X. J. Li, R. B. Wen, Y. Zhang, L. R. Zhu, B. L. Zhang and H. Q. Zhang, *J. Mater. Chem.*, 2009, **19**, 236.
24 O. Prucker, C. A. Naumann, J. Ruhe, W. Knoll and C. W. Frank, *J. Am. Chem. Soc.*, 1999, **121**, 8766.
25 A. Komp, J. Ruhe and H. Finkelmann, *Macromol. Rapid Commun.*, 2005, **26**, 813.
26 P. Beyer, L. Braun and R. Zentel, *Macromol. Chem. Phys.*, 2007, **208**, 2439.
27 S. Krause, R. Dersch, J. H. Wendorff and H. Finkelmann, *Macromol. Rapid Commun.*, 2007, **28**, 2062.
28 M. H. Li, P. Keller, J. Y. Yang and P. A. Albouy, *Adv. Mater.*, 2004, **16**, 1922.
29 M. Brehmer, R. Zentel, G. Wagenblast and K. Siemensmeyer, *Macromol. Chem. Phys.*, 1994, **195**, 1891.
30 E. Gebhard and R. Zentel, *Macromol. Rapid Commun.*, 1998, **19**, 341.
31 T. Ikeda, M. Nakano, Y. L. Yu, O. Tsutsumi and A. Kanazawa, *Adv. Mater.*, 2003, **15**, 201.
32 C. L. van Oosten, C. W. M. Bastiaansen and D. J. Broer, *Nat. Mater.*, 2009, **8**, 677.
33 T. Ikeda, J. I. Mamiya and Y. Yu, *Angew. Chem., Int. Ed.*, 2007, **46**, 506.
34 Y. Yu and T. Ikeda, *Macromol. Chem. Phys.*, 2005, **206**, 1705.
35 L. Cui, X. Tong, X. Yan, G. Liu and Y. Zhao, *Macromolecules*, 2004, **37**, 7097.
36 G. A. Shandryuk, S. A. Kuptsov, A. M. Shatalova, N. A. Plate and R. V. Talroze, *Macromolecules*, 2003, **36**, 3417.
37 L. Cui and Y. Zhao, *Chem. Mater.*, 2004, **16**, 2076.
38 S. V. Ahir, A. R. Tajbakhsh and E. M. Terentjev, *Adv. Funct. Mater.*, 2006, **16**, 556.
39 C. Ohm, C. Serra and R. Zentel, *Adv. Mater.*, 2009, **21**, 4859.
40 C. Ohm, N. Kapernaum, D. Nonnenmacher, F. Giesselmann, C. Serra and R. Zentel, *J. Am. Chem. Soc.*, 2011, **133**, 5305.
41 C. Ohm, M. Morys, F. R. Forst, L. Braun, A. Eremin, C. Serra, R. Stannarius and R. Zentel, *Soft Matter*, 2011, **7**, 3730.
42 E. Gebhard and R. Zentel, *Macromol. Chem. Phys.*, 2000, **201**, 902.
43 E. Gebhard and R. Zentel, *Macromol. Chem. Phys.*, 2000, **201**, 911.
44 M. Schadt, H. Seiberle, A. Schuster and S. M. Kelly, *Jpn. J. Appl. Phys.*, 1995, **34**, 3240.
45 M. Schadt, H. Seiberle, A. Schuster and S. M. Kelly, *Jpn. J. Appl. Phys.*, 1995, **34**, L764.
46 H. Finkelmann, S. T. Kim, A. Munoz, P. Palffy-Muhoray and B. Taheri, *Adv. Mater.*, 2001, **13**, 1069.
47 J. Reibel, M. Brehmer, R. Zentel and G. Decher, *Adv. Mater.*, 1995, **7**, 849.
48 H. M. Brodowsky, U. C. Boehnke, F. Kremer, E. Gebhard and R. Zentel, *Langmuir*, 1999, **15**, 274.
49 R. Stannarius, R. Kohler, U. Dietrich, M. Losche, C. Tolksdorf and R. Zentel, *Phys. Rev. E: Stat., Nonlinear, Soft Matter Phys.*, 2002, **65**, 041707.
50 R. Stannarius, R. Kohler, M. Rossle and R. Zentel, *Liq. Cryst.*, 2004, **31**, 895.
51 H. Schuring, R. Stannarius, C. Tolksdorf and R. Zentel, *Macromolecules*, 2001, **34**, 3962.
52 R. Stannarius, H. Schuring, C. Tolksdorf and R. Zentel, *Mol. Cryst. Liq. Cryst.*, 2001, **364**, 305.
53 C. H. Legge, F. J. Davis and G. R. Mitchell, *J. Phys. II*, 1991, **10**, 1253.
54 P.-G. de Gennes and C. R. Seances, *Acad. Sci., Ser. B*, 1975, **281**, 101.
55 H. Wermter and H. Finkelmann, *e-Polym.*, 2001, 013.
56 S. M. Clarke, A. Hotta, A. R. Tajbakhsh and E. M. Terentjev, *Phys. Rev. E: Stat. Phys., Plasmas, Fluids, Relat. Interdiscip. Top.*, 2001, **64**, 061702.
57 G. N. Mol, K. D. Harris, C. W. M. Bastiaansen and D. J. Broer, *Adv. Funct. Mater.*, 2005, **15**, 1155.
58 S. Saikrasun, S. Bualek-Limcharoen, S. Kohjiya and K. Urayama, *J. Polym. Sci., Part B: Polym. Phys.*, 2005, **43**, 135.
59 A. Buguin, M.-H. Li, P. Silberzan, B. Ladoux and P. Keller, *J. Am. Chem. Soc.*, 2006, **128**, 1088.
60 H. Yang, G. Ye, X. Wang and P. Keller, *Soft Matter*, 2011, **7**, 815.
61 J. Küpfer and H. Finkelmann, *Macromol. Chem. Phys.*, 1994, **195**, 1353.

62 M. Warner, K. P. Gelling and T. A. Vilgis, *J. Chem. Phys.*, 1988, **88**, 4008.
63 Y. Mao, E. M. Terentjev and M. Warner, *Phys. Rev. E: Stat. Phys., Plasmas, Fluids, Relat. Interdiscip. Top.*, 2001, **64**, 041803.
64 O. Stenull and T. C. Lubensky, *Phys. Rev. Lett.*, 2005, **94**, 018304.
65 M. Warner and E. M. Terentjev, *Prog. Polym. Sci.*, 1996, **21**, 853.
66 A. Sánchez-Ferrer, T. Fischl, M. Stubenrauch, H. Wurmus, M. Hoffmann and H. Finkelmann, *Macromol. Chem. Phys.*, 2009, **210**, 1671.
67 A. Sánchez-Ferrer, T. Fischl, M. Stubenrauch, A. Albrecht, H. Wurmus, M. Hoffmann and H. Finkelmann, *Adv. Mater.*, 2011, **23**, 4526.
68 H. Yang, A. Buguin, J. M. Taulemesse, K. Kaneko, S. Mery, A. Bergeret and P. Keller, *J. Am. Chem. Soc.*, 2009, **131**, 15000.
69 F. Ercole, T. P. Davis and R. A. Evans, *Polym. Chem.*, 2010, **1**, 37.
70 G. S. Kumar and D. C. Neckers, *Chem. Rev.*, 1989, **89**, 1915.
71 M. Irie, *Adv. Polym. Sci.*, 1990, **94**, 27.
72 T. Kinoshita, *J. Photochem. Photobiol., B*, 1998, **42**, 12.
73 C. Li, C.-W. Lo, C. Li, D. Zhu, Y. Liu and H. Jiang, *Macromol. Rapid Commun.*, 2009, **30**, 1928.
74 H. Finkelmann, E. Nishikawa, G. G. Pereira and M. Warner, *Phys. Rev. Lett.*, 2001, **87**, 015501.
75 Y. Yu, M. Nakano and T. Ikeda, *Nature*, 2003, **425**, 145.
76 S. V. Serak, N. V. Tabiryan, T. J. White and T. J. Bunning, *Opt. Express*, 2009, **17**, 15736.
77 M. Chen, X. Xing, Z. Liu, Y. Zhu, H. Liu, Y. Yu and F. Cheng, *Appl. Phys. A: Mater. Sci. Process.*, 2010, **100**, 39.
78 S. Xu, H. Ren, Y.-J. Lin, M. G. J. Moharam, S.-T. Wu and N. Tabiryan, *Opt. Express*, 2009, **17**, 17590.
79 M. Yamada, M. Kondo, J. Mamiya, Y. Yu, M. Kinoshita, C. J. Barrett and T. Ikeda, *Angew. Chem., Int. Ed.*, 2008, **47**, 4986.
80 M. Camacho-Lopez, H. Finkelmann, P. Palffy-Muhoray and M. Shelley, *Nat. Mater.*, 2004, **3**, 307.
81 M. Yamada, M. Kondo, R. Miyasato, Y. Naka, J. Mamiya, M. Kinoshita, A. Shishido, Y. Yu, C. J. Barrett and T. Ikeda, *J. Mater. Chem.*, 2009, **19**, 60.
82 F. Cheng, R. Yin, Y. Zhang, C.-C. Yen and Y. Yu, *Soft Matter*, 2010, **6**, 3447.
83 S. Serak, N. Tabiryan, R. Vergara, T. J. White, R. A. Vaia and T. J. Bunning, *Soft Matter*, 2010, **6**, 779.
84 R. Yin, W. Xu, M. Kondo, C.-C. Yen, J. Mamiya, T. Ikeda and Y. Yu, *J. Mater. Chem.*, 2009, **19**, 3141.
85 Y. Ji, J. E. Marshall and E. M. Terentjev, *Polymers*, 2012, **4**, 316.
86 S. Iijima, *Nature*, 1991, **354**, 56.
87 S. N. Kim, J. F. Rusling and F. Papadimitrakopoulos, *Adv. Mater.*, 2007, **19**, 3214.
88 W. Y. Zhou, X. D. Bai, E. G. Wang and S. S. Xie, *Adv. Mater.*, 2009, **21**, 4565.
89 M. A. Hamon, M. E. Itkis, S. Niyogi, T. Alvaraez, C. Kuper, M. Menon and R. C. Haddon, *J. Am. Chem. Soc.*, 2001, **123**, 11292.
90 L. Yang, K. Setyowati, A. Li, S. Gong and J. Chen, *Adv. Mater.*, 2008, **20**, 2271.
91 Y. Ji, Y. Huang, R. Rungsawang and E. M. Terentjev, *Adv. Mater.*, 2010, **22**, 3436.
92 C. Li, Y. Liu, C.-W. Lo and H. Jiang, *Soft Matter*, 2011, **16**, 7511.
93 N. Torras, K. E. Zinoviev, J. E. Marshall, E. M. Terentjev and J. Esteve, *Appl. Phys. Lett.*, 2011, **99**, 254102.
94 J. E. Marshall, Y. Ji, N. Torras, K. Zinoviev and E. M. Terentjev, *Soft Matter*, 2012, **8**, 1570.
95 C. J. Camargo, H. Campanella, J. E. Marshall, N. Torras, K. Zinoviev, E. M. Terentjev and J. Esteve, *Macromol. Rapid Commun.*, 2011, **32**, 1953.
96 C. Li, Y. Liu, X. Huang and H. Jiang, *Adv. Funct. Mater.*, 2012, **22**, 5166.
97 M. Kondo, M. Sugimoto, M. Yamada, Y. Naka, J. Mamiya, M. Kinoshita, A. Shishido, Y. Yu and T. Ikeda, *J. Mater. Chem.*, 2010, **20**, 117.
98 X. Sun, W. Wang, L. Qiu, W. Guo, Y. Yu and H. Peng, *Angew. Chem., Int. Ed.*, 2012, **51**, 8520.

